Supplementary Information

Engineering and Characterization of Fluorogenic Glycine Riboswitches

Simon Ketterer[1,2], Lukas Gladis[1,2], Adnan Kozica[1,2] and Matthias Meier[1,2,*]

[1]Microfluidic and Biological Engineering, Department of Microsystems Engineering - IMTEK, University of Freiburg, Georges-Koehler-Allee 103, 79110 Freiburg, Germany
[2]Centre for Biological Signalling Studies - BIOSS, University of Freiburg, Schänzlestrasse 18, 79104 Freiburg, Germany

* Correspondence should be addressed to: matthias.meier@imtek.de

Index

Methods

Figures

Tables

METHODS

Microfluidic chip production and workflow for building up pull-down assay

Polydimethylsiloxane (PDMS) chips were manufactured following the standard procedure for multilayer devices (Unger 2002). In short, control and flow molds were fabricated by using SU-8 3025 (MicroChem, USA) and AZ 9260 (MicroChemicals, Germany), respectively. The feature height of the control mold was 25±1 μm and 18±1 μm for the flow mold. PDMS (Sylgard 184, from Dow Corning, USA) was cast onto both molds and cured for 20 min at 80°C. Bonding between the flow and control PDMS layers was achieved by using an off-ratio method. Assembled PDMS devices were aligned to the spotted epoxy-coated glass slide and thermally bonded on a hot plate for 6 h at 80ºC.

Automated perfusion and actuation operations on chip included the following sequential steps (Figure S1B): (1) Coating of the epoxy-coated glass slide with biotinylated BSA 1 mg/mL in PBS (Thermo Scientific, Germany). (2) Deposition of NeutrAvidin 0.5 mg/mL in PBS (Thermo Scientific, Germany). (3) Actuation of the membrane valve that protects a circular area (80 μm diameter) of the pull-down chamber during the passivation step by flushing biotinylated BSA, (Meier, Maerkl). (4) Lift off of the button valve during perfusion of 10 μM capture DNA that is biotinylated at 3' end (Sigma Aldrich, Germany). (5) Introduction of the *in vitro* transcription (IVT) solution (HiScribe T7 High YieldRNASynthesis Kit, NewEngland Biolabs, USA) into the 640 microchambers containing the DNA spots. The transcription of Spinach DNA mutants was initiated upon heating to 37°C for 2 h using an ITO heating glass slide (Tokai Hit, Japan). (6) Transcribed Spinach mutant RNAs were allowed to diffuse to the pull-down area in the separated unit cells. (7) Synthetized riboswitches were pulled down to the capture DNA. (8) Washing of nonhybridized RNAs from the unit cells with detection buffer. Workflow of the thermodynamic and kinetic experiments is presented in Figure S1C.

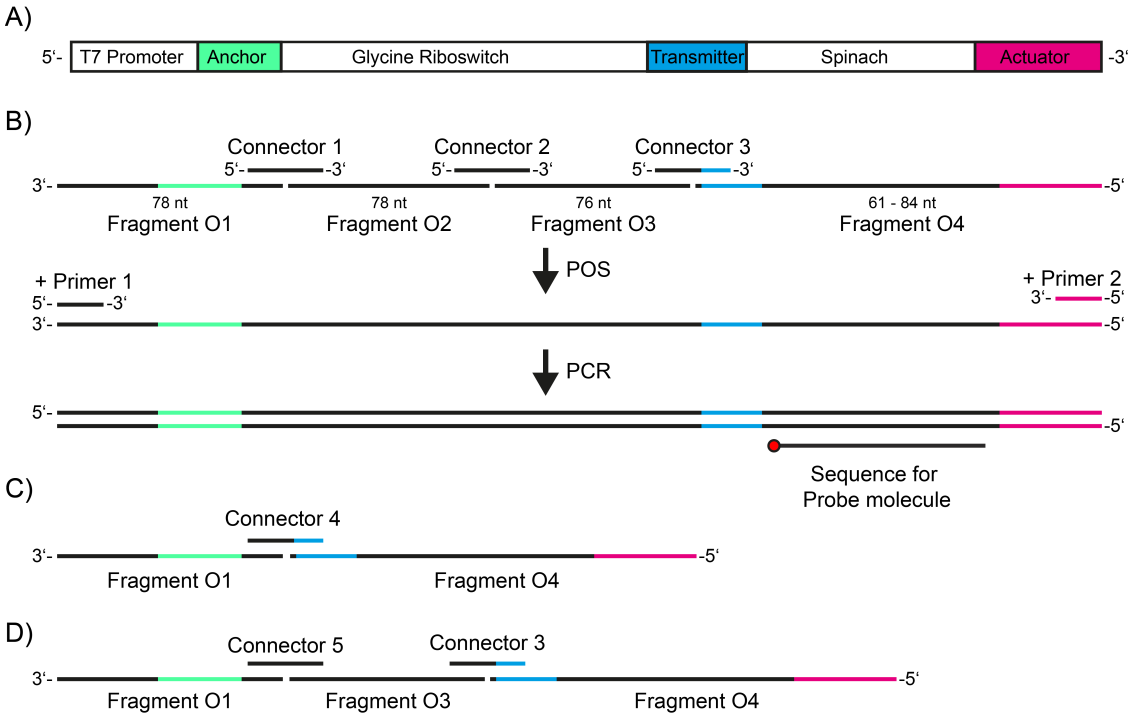

Figure S1. Schematic of the patch oligonucleotide synthesis (POS) used to generate fluorogenic glycine riboswitches. **A)** Sequence design of a fluorogenic glycine riboswitch for functional screening on a microfluidic chip. The variable transmitter is indicated in blue, the variable actuator sequence is indicated in pink, and the pull-down anchor is indicated in green. **B)** POS synthesis reaction scheme of the fluorogenic glycine riboswitches for the screening library. All corresponding sequences are given in table S1. **C)** POS of the negative control riboswitches without the glycine sensor aptamers. **D)** POS of the fluorogenic glycine riboswitch truncated by Gly-Apt-1.

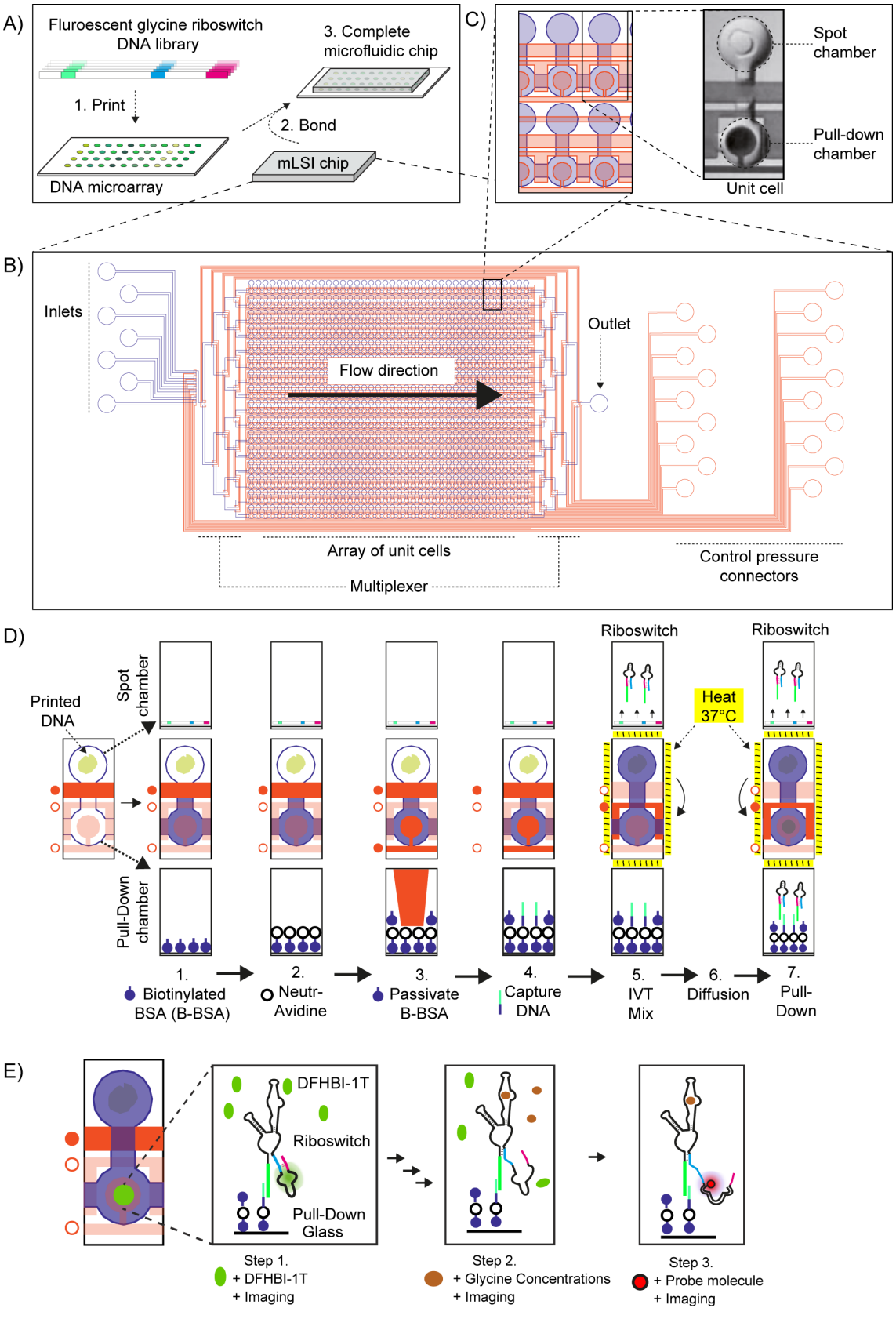
A)
Fluroescent glycine riboswitch DNA library
3. Complete microfluidic chip
1. Print
2. Bond
DNA microarray
mLSI chip
C)
Spot chamber
Pull-down chamber
Unit cell
B)
Inlets
Outlet
Flow direction
Array of unit cells
Multiplexer
Control pressure connectors
D)
Printed DNA
Spot chamber
Pull-Down chamber
Riboswitch
Riboswitch
Heat 37°C
1. Biotinylated BSA (B-BSA)
2. Neutr-Avidine
3. Passivate B-BSA
4. Capture DNA
5. IVT Mix
6. Diffusion
7. Pull-Down
E)
DFHBI-1T
Riboswitch
Pull-Down Glass
Step 1.
+ DFHBI-1T
+ Imaging
Step 2.
+ Glycine Concentrations
+ Imaging
Step 3.
+ Probe molecule
+ Imaging

Figure S2. Microfluidic chip-based workflow for functional screening and biophysical characterization of riboswitches. A) The DNA library was printed onto an epoxy-coated microscope slide. The PDMS-based microfluidic large-scale integration chip platform was then aligned and bonded to the microarray. B) Overall design and mLSI control elements of the microfluidic chip to test biomolecular interactions where control and flow channels are colored in red and blue, respectively. The chip has been previously published and described in its general functionality (20,23,31). C) Operational unit cell of the mLSI chip. One unit cell is separated by a pneumatic membrane valve into two microchambers with a volume of 1 nL. After alignment to the microarray, the top chamber contains the DNA spot of a riboswitch construct. Within the bottom chamber, the pull-down assay is built up. D) Chemical work program, which was automated and parallelized for all unit cells on chip. Within the cartoon, the red line denotes the pneumatic membrane valves where the open and closed small circle at the side of each panel denote open and closed valve states, respectively. Additionally, closed and open valves in the panels are marked with dark and light red, respectively. Fluids are highligthed in blue. Symbols for the surface pull-down are given in the panels. The fluidic workprogram Step 1 and 2: Build up of the pull-down assay within the assay chamber. For this, biotinylated BSA and NeutrAvidin are sequentially introduced with buffer flushing in between. Step 3: The button valve is closed and the biotinylated BSA is flushed to passivate all NeutrAvidin molecules outside the button area. Step 4: A biotinylated capture probe is deposited on the pull-down area by lifting the button valve. Step 5: The *in vitro* transcription solution is introduced and guided into the spot chamber. Step 6: The chip is heated on a thermoplate to 37°C for 2 hours (yellow box in the panel). During this step, the unit cells are separated and free diffusion of the syntheized RNA between the spot and pull-down chamber can occur. Step 7: Hybridization of the riboswitches to the pull-down anchor. E) On chip operations for determining apparent thermodynamic and kinetic parameters of the fluorogenic glycine riboswitches in response to glycine. Step 1: After the riboswitches are produced and pulled down to the surface of each unit cell, the detection buffer with DFHBI-1T is introduced. All unit cells are imaged. Step 2: The glycine concentration is increased sequentially within the unit cells. After each concentration step, the unit cells are imaged. In case kinetic parameters are measured, real time imaging of each unit cell is performed. Step 3: For determination of the riboswitch concentration on the pull-down area, the detection probe against the actuator is introduced. The chip is once more imaged. All required chemicals and concentrations to establish the miniaturized pull-down are given in the methods and matrials section.

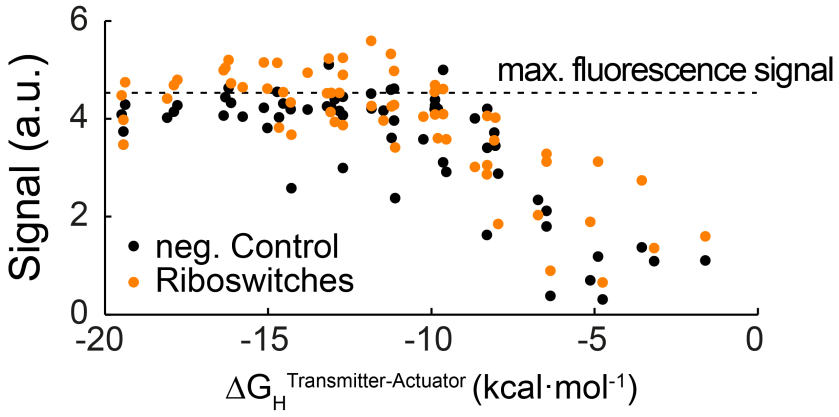

Figure S3. Fluorescence signal of the fluorogenic glycine riboswitches and the negative control constructs (without Gly-Apt-1 and 2) plotted against their theoretical hybridization energy (ΔG_H) of the transmitter/actuator strand. The maximal possible Spinach/DFHBI-1T fluorescence signal (dashed line) was obtained for fluorogenic glycine riboswitch design with a transmitter/actuator pair exhibiting ΔG_H larger -10 kcal/mol. Measurements were made within the detection buffer without glycine.

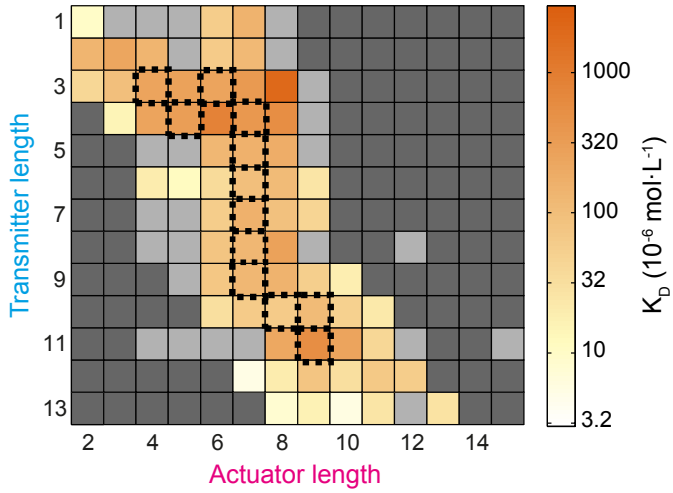

Figure S4. The apparent glycine dissociation constants (K_D) of the fluorogenic glycine riboswitch screened on chip. K_D values are plotted in dependence of the transmitter/actuator chain lengths of the riboswitches. The top 12 fluorogenic riboswitches with the highest ΔS from figure 2B are indicated by dotted border lines. Grey squares indicating non-measured values.

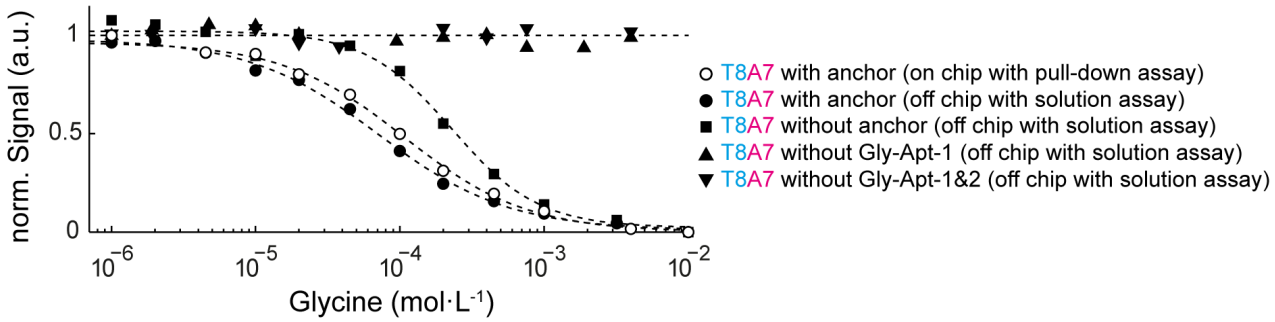

Figure S5. Comparison of the florescence signals obtained for the fluorogenic glycine riboswitch T8A7 on and off chip. The experiment shows that miniaturization and pull-down technology on chip did not alter the binding response of the fluorogenic glycine riboswitch.

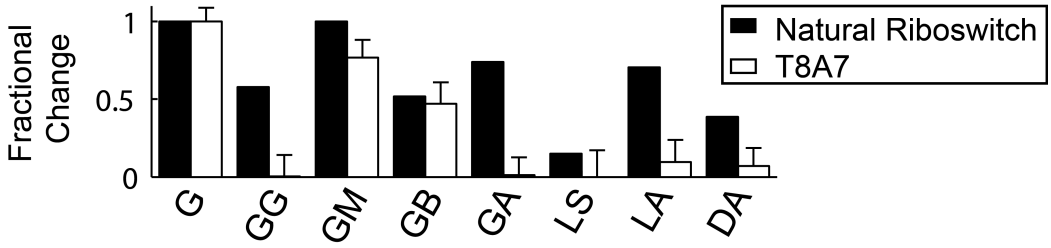

Figure S6. Specificity of the fluorogenic glycine riboswitch T8A7 compared to the natural glycine riboswitch. The open bars shows the fractional fluorescence signal change of the glycine upon addition of 10 mM glycine (G), glycyl-glycine (GG), glycine methyl ester (GM), glycine tert-butyl ester (GB), glycinamide (GA), L-serine (LS), L-alanine (LA), D-alanine (DA). The fractional change is normalized to the induced fluorescence change of the riboswitch by glycine. The closed bars show the fraction of early-terminated mRNAs to full-length transcribed mRNAs of a control gene containing the natural riboswitch sequence at the 5' UTR region measured within a single-round transcription assay. The compared data set is taken from Mandal *et al*. (5).

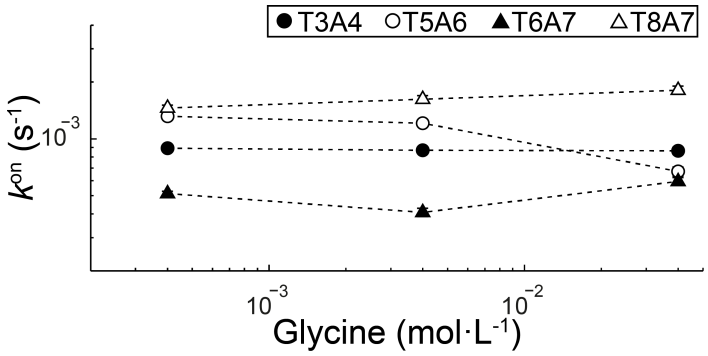

Figure S7. Representative apparent on-rates of glycine binding to four fluorogenic glycine riboswitch with different transmitter/actuator chain length in dependence of the glycine concentration.

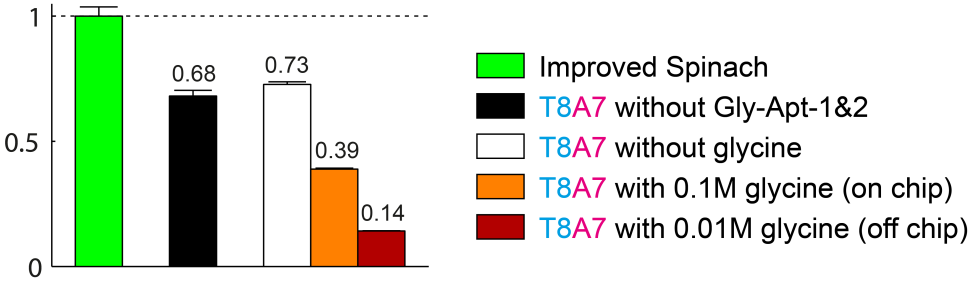

Figure S8. Normalized fluorescence signal change of the fluorogenic glycine riboswitch with a transmitter/actuator sequence of T8A7 compared to the improved wild type Spinach sequence. Values were recorded at 28°C.

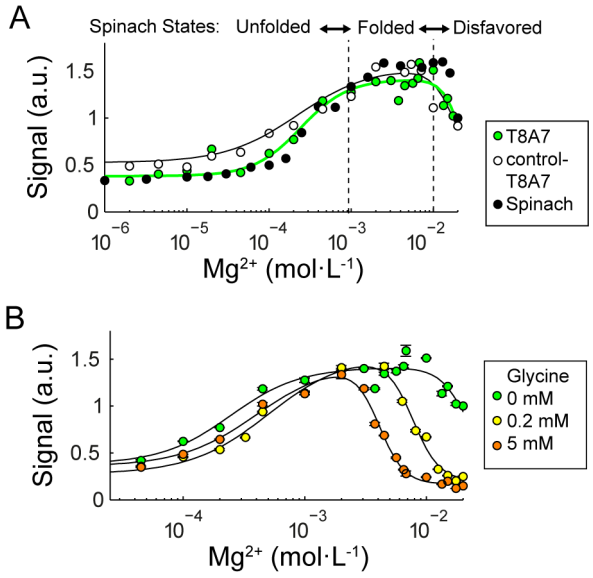

Figure S9. Magnesium dependency of the T8A7 fluorogenic glycine riboswitch. **A**) The magnesium dependency of the fluorescence signal intensity of the T8A7 glycine riboswitch, the negative control construct of T8A7, and Spinach (Ketterer et al. improved Spinach version) in absence of glycine. All three fluorogenic RNAs show a three state fluorescence response to the magnesium concentration. 1. The unfolded (*U*) state: At low magnesium concentration, no fluorescence signal can be detected for any construct. This is due to the fact that Spinach requires for folding its fluorogenic structure a low milimolar magnesium concentration (10). 2) The folded (*F*) state: From 0.1 mM magnesium in the detection buffer Spinach starts to form its functional fluorogenic structure. Most importantly, between a magnesium concentration of 1 to 10 mM the fluorescence signal of Spinach and the Spinach actuator within the negative and positive T8A7 riboswitch in absence of glycine was constant. 3) The disfavored (*D*) state: At magnesium concentrations higher than 10 mM the fluorescence of the negative and positive T8A7 riboswitch is decreasing. The reason for this decrease is unclear; however, it was also observed for the used Spinach version at a magnesium concentration of 20 mM and, thus, not caused by the glycine riboswitch. **B**) The magnesium dependency of glycine binding to the T8A7 fluorogenic riboswitch. For obtaining the magnesium binding constants to the T8A7 riboswitch at different glycine concentrations, we used the descriptive three state model from A), combining the $[U]$, $[F]$, and $[D]$ states of the Spinach actuator. It is expected that the glycine concentration shifts the Spinach actuator within the riboswitch from the folded into the unfolded state. Only the first two states contribute to a fluorescence signal, where the signal (S) of the *F* state outnumbers the signal of the *U* state. Thus, the measured fluorescence distribution is the quotient of $(S_U \cdot [U] + S_S \cdot [S])$ of the total RNA amount $([U] + [S] + [D])$. With the magnesium concentration $[M]$, the magnesium dissociation constants K_{D1} and K_{D2} (one for each transition), the corresponding Hill coefficients (h_1 and h_2) and the fluorescence background signal in absence of magnesium (S_B), the fluorescence curve be described with the following equation:

$$S([M]) = \frac{S_U + S_F \cdot ([M]/K_{D1})^{h_1}}{1 + ([M]/K_{D1})^{h_1} \cdot (1 + ([M]/K_{D2})^{h_2})} + S_B$$

By fitting the model to the data in B), we obtained the following parameters:

Glycine / mM	K_{D1}/ µM	K_{D2} / mM	h_1	h_2
0	230±40	15.8±1.1	1.8±0.5	7±3
0.2	420±50	8.3±0.4	1.7±0.3	4.3±0.9
5	390±130	4.2±0.2	1.5±0.5	4.3±0.9

All measurements were taken at 28°C in detection buffer with the in-solution assay. All values are normalized to the fluorescence signal at 20 mM magnesium in the absence of glycine. 20 mM magnesium was used for all measurements in the manuscript.

Table S1. Oligonucleotide sequences for the synthesis of fluorogenic glycine riboswitches. The sequence for the variable fragment O4 and corresponding connector C3 and primer P2 is representative of the riboswitch with the actuator (bold), transmitter (underlined), and minimal Spinach (italic) sequence of the fluorogenic glycine riboswitch T13A13. For construction of all fluorogenic riboswitche only the transmitter/actuator pairs have to be exchanged.

Label	**Sequence**	**Modification**
Fragment O1	GTCTCTCCCCTTGCTGTCATTCGCTCATATCTTGTGTTATTATTTTGA ATGTTTGTTCCCCTATAGTGAGTCGTATTAGCG	5'-Phos
Fragment O2	GAGCAAGAGTTCTTTTGCCTGAGAGATTCACTCCGCAGTTTGCTCC TTCGGCGCCTGTATCCCGAGGTTTTCGGTCAG	5'-Phos
Fragment O3	AAGTTTACTTTGCATACGCAAAGACGTCCCCTTTGGTGGTTTGCGC ATCCGCACAAACACTCTCCAGAGTTGCGTC	5'-Phos
Example: Fragment O4 for T13A13	**CAGAGAACCGGAG***CTCACACTCTACTCAACAGCTGCCGAAGCAGC TGGACCCGTCCTT*<u>CTCCGGTTCTCTG</u>TCCTGGCACCTGA	
Connector C1	CGAATGACAGCAAGGGGAGAGACCTGACCGAAAACCTCGGGATA CA	
Connector C2	CTCAGGCAAAAGAACTCTTGCTCGACGCAACTCTGGAGAGTGTTT	
Example: Connector C3 for T13A13	CTTTGCGTATGCAAAGTAAACTTTCAGGTGCCAGGACAGAGAAC	
Primer 1	CGCTAATACGACTCACTATAGGGGAACA	
Example: Primer 2 for T13A13	CAGAGAACCGGAGCTCACACT	
Capture DNA	TTGTGTTATTATTTTGAATGTTTGTTCCCC	3'-BtnTg
Spinach probe	CACACTCTACTCAACAGCTGCCGAAGCAGCTGGACCCGTCC	3'-ROX
Example: Connector 4 (negative control T13A13)	CGAATGACAGCAAGGGGAGAGACTCAGGTGCCAGGACAGAGAAC	
Fragment O1 for -Gly-Apt1 control	CTTTTTTTGTGTTATTATTTTGAATGTTTGTTCCCCTATAGTGAGTCG TATTAGCG	5'-Phos
Connector 5	CAAAATAATAACACAAAAAAAGGACGCAACTCTGGAGAGTGTTT	

Table S2. Transmitter and actuator sequences. The actuator sequence is given for the longest construct. In cases where the actuator sequence was longer than the transmitter, the actuator was designed to fold back to the 5' adjacent sensor bases. Riboswitches with actuator version T6* was characterized and all thermodynamic values adde to Table S3. The T6* transmitter exhibits a higher GC content as T6 and thus resembles more closely the T8 constructs.

Sensor sequence	Label	Transmitter sequences	Label	Actuator Sequence
GCCAGGA	T1	C	A8	GUCCUGGC
GCCAGGA	T2	CA	A8	UGUCCUGG
GCCAGGA	T3	CAG	A9	CUGUCCUGG
GCCAGGA	T4	CAGA	A9	UCUGUCCUG
GCCAGGA	T5	CAGAG	A9	CUCUGUCCU
GCCAGGA	T6	CAGAGA	A9	UCUCUGUCC
GCCAGGA	T6*	CAGAGG	A9	CCUCUGUCC
GCCAGGA	T7	CAGAGAG	A9	CUCUCUGUC
GCCAGGA	T8	CAGAGAAG	A11	CUUCUCUGUCCU
GCCAGGA	T9	CAGAGAAAG	A10	CUUUCUCUGU
GCCAGGA	T10	CAGAGAAGAG	A11	CUCUUCUCUGU
GCCAGGA	T11	CAGAGAAGGAG	A15	CUCCUUCUCUGUCCU
GCCAGGA	T12	CAGAGAACGGAG	A12	CUCCGUUCUCUG
GCCAGGA	T13	CAGAGAACCGGAG	A13	CUCCGGUUCUCUG

Table S3. Summary of all thermodynamic and kinetic parameters measured for the generated fluorogenic glycine riboswitch library. The table is added as text file.

Table S4. Comparision of the thermodynamic glycine binding parameters of fluorogenic riboswitches with and without anchor sequence. In both series the binding constant is increasing linearly with longer actuator length.

Riboswitch	+ Anchor Seq. On Chip Assay		- Anchor Seq In Solution Assay	
	K_D / µM	*h*	K_D / mM	*h*
T8A6	79.7±7	1.3	121 ± 17	1.55
T8A7	125.8±4	0.9	231 ± 32	1.5
T8A8	273.9±48	0.4	450 ± 55	1.3
T8A9	not functional		not functional	